Separation Science and Technology
Publication details, including instructions for authors and subscription information:
http://www.informaworld.com/smpp/title~content=t713708471

A Study on Concentration Polarization in Ultrafiltration

S. Ilias[a]; R. Govind[b]
[a] Department of Chemical Engineering, North Carolina A&T State University, Greensboro, NC [b] Department of Chemical Engineering, University of Cincinnati, Cincinnati, OH

To cite this Article Ilias, S. and Govind, R.(1993) 'A Study on Concentration Polarization in Ultrafiltration', Separation Science and Technology, 28: 1, 361 — 381
To link to this Article: DOI: 10.1080/01496399308019495
URL: http://dx.doi.org/10.1080/01496399308019495

SEPARATION SCIENCE AND TECHNOLOGY, 28(1-3), pp. 361-381 (1993)

A STUDY ON CONCENTRATION POLARIZATION IN ULTRAFILTRATION

S. Ilias*
Department of Chemical Engineering
North Carolina A&T State University
Greensboro, NC 27411

R. Govind
Department of Chemical Engineering
University of Cincinnati
Cincinnati, OH 45221

ABSTRACT

A finite-difference solution of coupled transport equations for momentum and solute continuity is presented to model the concentration polarization in a tubular ultrafiltration (UF) system. The model includes the effects of solute osmotic pressure and solute rejection at the membrane surface, axial pressure drop and resistance of the gel layer. This provides a fundamental understanding of the dynamics of various operating parameters on concentration polarization and transmembrane flux. Simulation results are presented for a wide range of operating variables to show their effects on local variation of solute concentration and transmembrane flux. The numerical results were also compared with previously published experimental data, which shows that a concentration polarization model based on constant membrane permeability (usually obtained from pure water flux data) grossly overestimates the flux behavior. If the effect of gel polarization is included, the model can predict the actual permeate flux very closely. Thus, in modeling ultrafiltration, one needs to be careful in using the appropriate membrane permeability terms. The commonly used intrinsic membrane permeability which is usually a constant, may not describe the true flux behavior in ultrafiltration. Actually the nature of the feed, solute-surface interaction and gel layer formation control the effective permeability, which varies axially along the membrane length.

* To whom correspondence should be addressed

INTRODUCTION

Ultrafiltration (UF) is a simple and convenient membrane filtration process for concentration, purification and separation of macromolecules, colloids and suspended particles from solutions. In recent years, due to advances in asymmetric membranes and improved module designs, UF systems have found wide acceptance in many industrial and laboratory applications (1). In many industrial applications UF systems are favored over other traditional separation methods due to their low energy requirement and athermal character. However, the decline of flux in UF processes still remains a major concern, which is attributed to 'concentration polarization' (CP) and membrane 'fouling' (2).

Concentration polarization is described as the build-up of solutes close to or on the membrane surface due to convective-diffusive transport of solutes in the boundary layer. This results in an increase in both resistance to solvent transport and the local osmotic pressure, which reduces the permeation rate. The operating parameters that usually affect concentration polarization are velocity, pressure, temperature and feed concentrations. On the other hand, fouling is the deposition and accumulation of suspended and colloidal particles on the membrane surface, including crystallization, precipitation or adsorption of solutes on the membrane surface and within the pores. This results in lowering of flux and/or increase in rejection of solutes. Fouling is usually an irreversible and time-dependent phenomenon, which distinguishes it from concentration polarization (3-5).

In membrane separation systems, it is difficult to distinguish the relative role of CP and fouling in observed flux decline, as both of them tend to lower the flux. It is known that in a UF system, the initial flux decline is generally attributed to rapid buildup of a fouling layer and then the flux approaches a constant, steady-state value. Such a flux decline may last from a few minutes to several hours depending on membrane materials, feed composition and operating conditions. Thus, an understanding of the mechanics of flux decline phenomena is important for both optimum operation and control of underlying causes for concentration polarization and fouling in UF system.

BACKGROUND

In order to analyze the problem of concentration polarization, one must understand the transport phenomena at the membrane-solute interface. In the past, numerous efforts have been made to develop models to predict concentration polarization and its effect on transmembrane flux. For modeling purposes, usually

a thin-channel (parallel plate) or tubular membrane module is considered as a model element. In most cases, model development starts with the fundamental equations of fluid flow and solute continuity, which are given as (6):

$$\frac{D\rho}{Dt} = -\rho\nabla\vec{v} \tag{1}$$

$$\rho\frac{D\vec{v}}{Dt} = -\nabla p - \mu\nabla^2\vec{v} \tag{2}$$

$$\frac{Dc}{Dt} = D_e\nabla^2 c \tag{3}$$

Equations 2 and 3 are non-linear elliptic equations which are coupled via wall permeation velocity and solute concentration at the membrane surface. These equations are equally applicable to reverse osmosis and ultrafiltration membrane processes. For solution of these PDE's, the boundary conditions on the entire solution domain are required to be specified, which are obviously not known a priori in UF systems. Thus to obtain analytical or numerical solution, one has to make use of some assumptions to simplify the equations which represent the phenomena.

Probably, Dresner (7), Fisher et al. (8), Sherwood et al. (9), Brian (10) and Gill et al. (11) are the first few investigators who attempted to analyze the concentration polarization in reverse osmosis using transport Eqs. 1-3. Dresner (7) analyzed the thin-channel problem under laminar flow conditions for a case of complete solute rejection and constant wall permeation flux. With these assumptions, the transport equations were decoupled and, using the velocity field given by Berman (12), Dresner (7) obtained an approximate solution for concentration polarization. Fisher et al. (9) modified Dresner's solution and applied it to tubular membranes. Sherwood et al. (9) solved the same problem as Dresner (7) using a Graetz-type analogy. Brian (10) studied the same system but with variable wall flux conditions. Assuming that the osmotic pressure is proportional to salt concentration and that the transmembrane pressure drop is insignificant, Brian obtained a concentration-dependent wall-permeation velocity. To solve the diffusion equation by a finite-difference method as a part of an iterative scheme, Brian used the fluid flow field given by Berman (12), but excluded the terms containing the wall Reynolds number. Gill et al. (11) also solved the same problem using a perturbation series solution.

Since then, a large number of analyses of concentration polarization in thin-channel and tubular modules have appeared (13-22). A review of these works indicates that, in general, the transport equations for ultrafiltration and/or reverse osmosis membranes are decoupled and simplified by assuming one or more of the following modifications:

1. The fluid flow field is approximated by some prescribed functions or by a reduced form of the momentum equation (usually some type of perturbation solution).
2. The wall permeation velocity is constant or piece-wise constant along the axial length.
3. The wall velocity may depend on osmotic pressure but axial pressure drop is neglected or an approximate pressure drop is used without solving the momentum equation.
4. Analysis of membrane permeability is never detailed; instead an effective permeability is usually used.
5. Usually constant fluid and transport properties are assumed. Some studies on the concentration dependence of viscosity and diffusivity on polarization have also been reported.

The above discussion reveals that previous modeling efforts were essentially based on the decoupling of the transport equations and some major simplifications of wall permeation boundary conditions. However, a rigorous concentration polarization model would require solution of coupled transport equations with wall permeation conditions which would depend on transmembrane pressure drop and solute concentration at the membrane interface. Thus, in this paper a revised model is presented which requires the solution of coupled transport equations along with appropriate wall permeation boundary conditions.

MODEL DEVELOPMENT

Consider a tubular ultrafilter membrane of radius r_i. L is the effective length of the module. The feed stream inside the tube is laminar, incompressible (constant density and viscosity) and solute diffusivity is assumed to be constant. Before we consider the appropriate transport equations, let us consider the local transmembrane flux, v_w, which is given by (23):

$$v_w = A_m(\Delta p - \Delta \pi) \tag{4}$$

For pure solvent as feed, v_w is proportional to transmembrane pressure drop, Δp and the membrane permeability, A_m is the proportionality constant. However, with feed solution, v_w may not only depend on Δp and $\Delta\pi$, but also strongly depends on A_m, which cannot be assumed constant for various reasons as discussed below.

In membrane filtration, following the resistance-in-series concept common in heat transfer, the permeability may be given by:

$$A_m = \frac{1}{r_{mw} + r_{mf} + r_p} \tag{5}$$

Here, r_{mw} is the intrinsic resistance of the membrane, which is usually a constant and may be obtained from pressure-flux data of pure water as feed. The average transmembrane flux, J is given as:

$$J = A_m \Delta p = \frac{\Delta p}{r_{mw}} \tag{6}$$

The pressure-flux relationship given by Eq. 6 is strictly applicable to clean, unfouled membrane. The resistance of the fouling layer, r_{mf}, which is due to build-up of deposits on the membrane surface, is responsible for observed flux decline. In ultrafiltration of macromolecules and dilute suspensions, the thickness of the fouling layer increases as filtration proceeds, resulting in decline of flux at constant pressure. Using the conventional filtration theory of particulates, one may approximate r_{mf}, the dynamic resistance, as:

$$r_{mf} = \frac{\phi w Q_t (\Delta p)^s \mu}{A} \tag{7}$$

If the resistance of the polarization layer, r_p, is assumed to be insignificant in absence of pore blockage, the flux is given by (24):

$$J = \frac{\Delta p}{\frac{\phi w Q_t \mu (\Delta p)^s}{A} + r_{mw}} \tag{8}$$

Equation 8 may be rearranged to give:

$$\frac{1}{J} = \frac{\phi w Q_t \mu (\Delta p)^{s-1}}{A} + \frac{r_{mw}}{\Delta p} \tag{9}$$

The previous equation suggests that a plot of 1/J vs Q_t for constant pressure filtration will yield a straight line. Thus, for a given system, from the slopes of two sets of data taken at different Δp, one may evaluate the independent constants ϕ and s, provided w, Q_t, μ, A, and Δp are known. With the known values of ϕ and s, the dynamic resistance can now be computed from Eq. 7. Although this analysis is more appropriate to microfiltration (24), there has been some reported success of this approach in ultrafiltration (25-28).

As discussed earlier, after the initial flux decline, it is the concentration polarization that dictates the transmembrane flux, which essentially remains constant during filtration. At this point, besides the resistances due to the membrane and the fouling layer, the resistance of the polarization layer needs to be accounted for in the flux calculation. The polarization layer resistance consists of two resistances: r_{pg} due to the gel polarized layer and $r_{p\delta}$ due to the associated boundary layer. The evaluation of these resistances is not straightforward. One commonly used approach is to use the film theory model, which is applicable only to the concentration boundary layer (29-31). Cheryan (1) suggested that r_p may be taken as a function of applied pressure, i.e.,

$$r_p = \Phi \Delta p \tag{10}$$

where, Φ is a function of the variables affecting the mass transfer properties of the system and may be obtained experimentally.

From their experimental study on polarization of polyvinyl alcohol (PVA) and ovalbumin aqueous solutions in ultrafiltration, Nakao et al. (32) reported that the resistance of the gel-polarized layer can be expressed as:

$$r_p = a_o c_g^{a_1} \tag{11}$$

where a_o is a proportionality constant,which depends on the type of macromolecules, while the power a_1 was found to be a constant independent of the kind of macromolecules, module geometry and operating conditions. The estimated value of a_1 was 1.7. The values of a_o for polyvinyl alcohol and ovalbumin are 1.961E05 and 4.413E04, respectively, when the resistance r_p in Eq. 11 is expressed in $kPa \cdot s \cdot cm^{-1}$.

From the above discussion, it is now clear that at present, we do not have appropriate models for all the resistances needed to compute transmembrane flux. However, it seems logical to overcome this difficulty by substituting an effective membrane resistance, r_m for r_{mw} and r_{mf}. Further, we can use Eq. 11 for the resistance of the gel-layer and, by including the osmotic-pressure effect for non-linear flux-pressure behavior, the flux can be related to:

$$J = \frac{\Delta p - \Delta \pi}{r_m + r_p} \tag{12}$$

Note that the flux given by the above equation is nothing but the average flux for a given ultrafiltration system. But, in a flow system such as a thin-channel or a tubular module, the concentration, c_g, and the osmotic and transmembrane pressure vary along the length of the module. Thus, for the system under consideration, we can use local flux as:

$$v_w = \frac{\Delta p - \Delta \pi}{r_m + r_p} \tag{13}$$

Since we intend to model concentration polarization in a tubular membrane module, we can use parabolic type transport equations instead of elliptic equations by using axisymmetric flow and boundary-layer type approximations. Thus, for this case the appropriate governing equations in dimensionless form are given as:

$$\frac{\partial U}{\partial Z} + \frac{1}{R}\frac{\partial}{\partial R}(RV) = 0 \tag{14}$$

$$U\frac{\partial U}{\partial Z} + V\frac{\partial U}{\partial R} = -\frac{1}{2}\frac{dP}{dZ} + \frac{1}{Re_{w0}}\left(\frac{\partial^2 U}{\partial R^2} + \frac{1}{R}\frac{\partial U}{\partial R}\right) \tag{15}$$

$$U\frac{\partial C}{\partial Z} + V\frac{\partial C}{\partial R} = \frac{1}{Pe_{w0}}\left(\frac{\partial^2 C}{\partial R^2} + \frac{1}{R}\frac{\partial C}{\partial R}\right) \tag{16}$$

The wall Reynolds number, Re_{w0} and Peclet number, Pe_{w0} are based on initial wall permeation velocity, v_{w0} and inside radius of the tubular membrane, r_i. The boundary conditions for Eqs. 14 to 16 are as follows:
At the inlet, Z = 0:

$$U(R,0) = U_0(R) = 2.0(1-R^2); \quad V(R,0) = 0; \quad C(R,0) = 1 \tag{17}$$

At the membrane wall, R = 1:

$$U(1,Z) = 0; \quad V(1,Z) = V_w(Z) = \frac{\Delta P - \Delta \Pi}{R_m + R_p}; \quad \left.\frac{\partial C}{\partial Z}\right|_{1,Z} = Pe_{w0}\beta V_w C_g \tag{18}$$

At the axis of symmetry, R = 0:

$$\left.\frac{\partial U}{\partial R}\right|_{0,Z} = 0; \qquad \left.\frac{\partial C}{\partial R}\right|_{0,Z} = 0 \tag{19}$$

The boundary conditions, Eq. 17 specify the inlet flow and concentration profiles. The inlet velocity profile may be either uniform (plug flow) or parabolic (Poiseuille flow). The concentration distribution of the feed solution at the inlet is assumed to be uniform. The boundary conditions at the membrane wall for the momentum and solute continuity equations is given by Eq. 18. No slip condition is assumed at the membrane surface. The momentum equation is coupled with the solute continuity equation by the wall flux and the solute mass balance of convective-diffusive transport at the membrane surface with solute rejection. The wall flux condition is determined by the axial transmembrane pressure drop, concentration-dependent local osmotic pressure drop across the membrane and membrane resistances. If the resistance of the gel-polarized layer is neglected in the wall flux condition, then the model may be referred to as the 'Concentration Polarization (CP) model'. Otherwise, the model may be regarded as the 'Gel-polarization (GP) model', where the resistance of the gel-polarized layer is given by Eq. 11, which depends on the local solute concentration at the membrane surface. Equation 19 assumes symmetry with respect to the centerline for axisymmetric flow and solute transport.

METHOD OF SOLUTION

Equations 14 to 16 are solved by a finite difference method implicit in R. A system of grid lines running in Z- and R-directions, i.e., i and j lines, are imposed on the solution domain. The axial grid lines are numbered from 1 to m, i.e., i=1 being the inlet boundary (Z=0), while i=m is the last axial grid line ($Z=Z_{max}$) of the solution domain. Similarly, transverse grid lines are numbered from 1 to n, where j=1, corresponds to the centerline (R=0) and the wall is matched at j=n (R=1). In the finite difference approximation, the convective terms $U(\partial U/\partial Z)$, $V(\partial U/\partial R)$, $U(\partial C/\partial Z)$, and $V(\partial C/\partial R)$ at interior grid point (i,j) were linearized by approximating the coefficients U and V at (i-1,j), i.e. by taking the known velocities at the previous grid point. The second-order derivative terms were approximated by a three-point centered difference scheme. Equation 14 was discretized by a centered difference scheme by taking the derivatives at (i,j-1/2). The derivative boundary conditions at the axis of symmetry were approximated by three-point forward difference, while the

derivative condition at the membrane surface was given by a three-point backward difference formula. These boundary conditions were used to compute U and C at the wall and center of the tube.

Following the above discretization schemes, finite difference approximations of Eqs. 14 to 16 are derived as follows:

$$V_{i,j} = -\sum_{j=2}^{n} \frac{(R_j - R_{j-1})(R_j + R_{j-1})}{4R_j \Delta Z}(U_{i,j} - U_{i-1,j} + U_{i,j-1} - U_{i-1,j-1}) \quad (20)$$

$$A_j U_{i,j-1} + B_j U_{i,j} + D_j U_{i,j+1} = E_j \qquad for \ \ 2 \le j \le n-1 \quad (21)$$

$$F_j C_{i,j-1} + G_j C_{i,j} + H_j C_{i,j+1} = I_j \qquad for \ \ 2 \le j \le n-1 \quad (22)$$

where

$$A_j = -\frac{DR1}{(DR)(DR2)}\left(V_{i-1,j} - \frac{1}{Re_{w0}R_j}\right) - \frac{2}{Re_{w0}(DR)(DR2)} \quad (23)$$

$$B_j = \frac{DR1 - DR2}{(DR2)(DR)}\left(V_{i-1,j} - \frac{1}{Re_{w0}R_j}\right) + \frac{2}{Re_{w0}(DR2)(DR1)} + \frac{U_{i-1,j}}{\Delta Z} \quad (24)$$

$$D_j = -\frac{DR2}{(DR1)(DR)}\left(V_{i-1,j} - \frac{1}{Re_{w0}R_j}\right) - \frac{2}{Re_{w0}(DR1)(DR)} \quad (25)$$

$$E_j = \frac{U_{i-1,j}^2}{\Delta Z} - \frac{1}{2}\left.\frac{dP}{dZ}\right|_{i,j} \quad (26)$$

$$F_j = -\frac{DR1}{(DR)(DR2)}\left(V_{i-1,j} - \frac{1}{Pe_{w0}R_j}\right) - \frac{2}{Pe_{w0}(DR)(DR2)} \quad (27)$$

$$G_j = \frac{DR1 - DR2}{(DR2)(DR)}\left(V_{i-1,j} - \frac{1}{Pe_{w0}R_j}\right) + \frac{2}{Pe_{w0}(DR2)(DR1)} + \frac{U_{i-1,j}}{\Delta Z} \quad (28)$$

$$H_j = -\frac{DR2}{(DR1)(DR)}\left(V_{i-1,j} - \frac{1}{Pe_{w0}R_j}\right) - \frac{2}{Pe_{w0}(DR1)(DR)} \tag{29}$$

$$I_j = U_{i-1,j}\frac{C_{i-1,j}}{\Delta Z} \tag{30}$$

with

$$DR = R_{j+1} - R_{j-1}; \quad DR1 = R_{j+1} - R_j; \quad DR2 = R_j - R_{j-1} \tag{31}$$

The derivative boundary conditions, Eqs. 18 and 19 are expressed as:

$$U_{i,1} = \frac{U_{i,2}(R_1 - R_3)^2 - U_{i,3}(R_1 - R_2)^2}{(R_2 - R_3)(2R_1 - R_2 - R_3)} \tag{32}$$

$$C_{i,1} = \frac{C_{i,2}(R_1 - R_3)^2 - C_{i,3}(R_1 - R_2)^2}{(R_2 - R_3)(2R_1 - R_2 - R_3)} \tag{33}$$

$$C_{i,n} = \frac{C_{i,n-1}(R_n - R_{n-2})^2 - C_{i,n-2}(R_n - R_{n-1})^2}{(R_{n-1} - R_{n-2})(2R_n - R_{n-1} - R_{n-2} - Pe_{w0}\beta V_{i,n}(R_n - R_{n-1})(R_n - R_{n-2}))} \tag{34}$$

An iterative procedure was developed to solve Eqs. 20 to 22 with necessary boundary conditions. The solution procedure is as follows:

1. The velocity and concentration profiles on the inlet plane (i=1 line) are specified. To compute the variables on the next line, i=2, a pressure gradient, dP/dZ and solute concentration at the wall, C_g are assumed.
2. The system of equations, Eq. 21 is solved by the Thomas algorithm which gives the U-velocity distribution. The V-velocity distribution is then computed from Eq. 20. However, this solution will not, in general, satisfy $V_{i,n}=V_w$, as required by the wall flux condition.

3. With a second guess of pressure gradient, step 2 is repeated to compute U- and V-velocity distribution. This solution may again not satisfy $V_{i,n}=V_w$ from guess of C_g.
4. Using the values of $V_{i,n}$ and pressure gradient in steps 2 and 3, an improved estimate of the pressure gradient that gives $V_{i,n} \approx V_w$, is found by linear interpolation.
5. Step 3 is repeated to obtain U- and V-velocity distribution. If the wall flux condition is not satisfied within a preset value, then a new improved value of pressure gradient is obtained by interpolating the values of $V_{i,n}$ and pressure gradient in steps 5 and 3 or 2. The iteration is continued till the convergence in wall flux condition is achieved.
6. With the converged flow field, Eq. 22 is solved to get the solute distribution on line i=2 and solute concentration on the membrane surface is obtained from Eq. 34. If the solute concentration $C_{i,n}$ is different from C_g by more than the preset tolerance limit, a new improved guess of C_g is obtained taking the average of the values.
7. With the new value of C_g, steps 2 to 6 are repeated until both the flow and concentration fields converge simultaneously.
8. Once the solutions on line i=2 are found, the above procedure (steps 1 to 7) is extended to next i-line and so on.

In this work, for convergence of flow and concentration fields, $|V_{i,n} - V_w| \leq 10^{-6}$ and $|C_{i,n} - C_g| \leq 10^{-6}$, were used as convergence criteria, respectively. No numerical difficulties were encountered in any of the simulation runs.

The finite difference method just described may be readily applied to thin-channel or hollow-fiber UF systems. The effects of concentration-dependent viscosity and solute diffusivity can be easily accommodated in the present numerical scheme with minor modifications in programming, provided their functional relationships are known as functions of solute concentration.

RESULTS AND DISCUSSION

In this paper, we have presented the simulation of concentration polarization in a tubular ultrafiltration membrane based on the solution of coupled transport equations. To broaden the understanding of various factors that affect the concentration polarization and transmembrane flux, numerical simulations were performed for a number of important operating and process variables. In all simulation runs, the dimension of the model ultrafiltration unit was 30 cm long and 1.25 cm diameter. PVA 224 aqueous solution was used as feed. A numerical

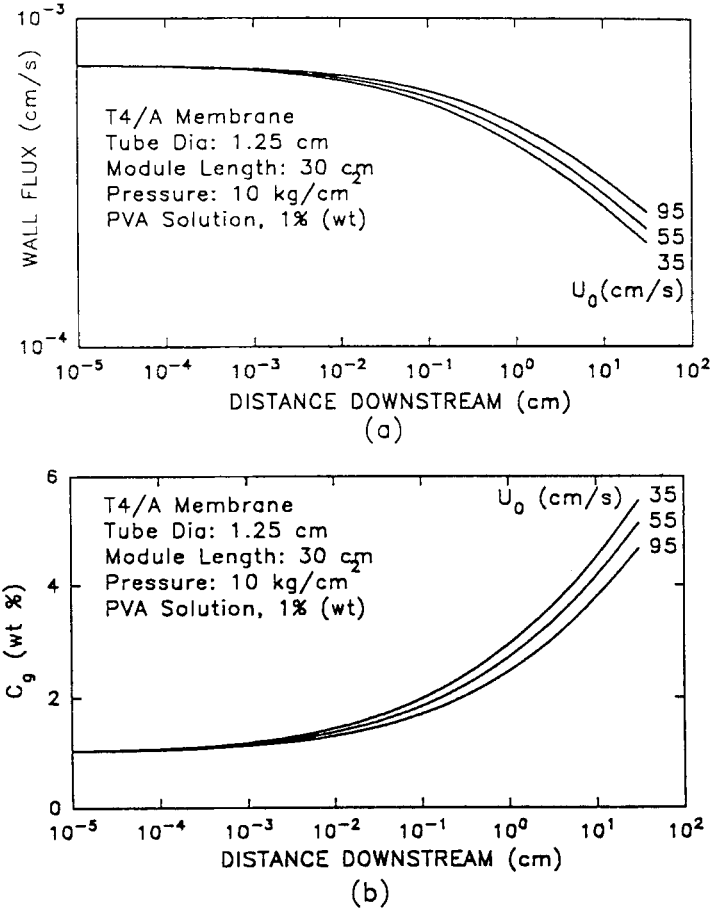

FIGURE 1: Axial variation of (a) transmembrane flux, and (b) solute concentration at the membrane wall with feed flow rate (u_o) as a parameter. Feed flow rates are 35, 55, and 95 cm/s.

value of 1.8E-07 $cm^2 \cdot s^{-1}$ was used as the diffusion coefficient (D_e) in all calculations. Due to non-availability of osmotic pressure data for PVA 224, the effect of osmotic pressure is neglected in this simulation work. This would result in a higher predicted flux. The gel polarization resistance for PVA 224 was estimated from the following equation (32):

$$r_p = 2.0E03c_g^{1.7} \tag{35}$$

The inlet velocity profile was assumed to be parabolic, which corresponds to the physical situation in which an impermeable tubular section is smoothly connected to the membrane unit and the impermeable section is of sufficient length to allow the development of fully developed flow. In the following sections, we briefly describe some of the important simulation results along with some available experimental data.

The important variables that affect the performance of a given UF system are: feed flow rates, operating pressure, feed concentration, viscosity and solute diffusivity. In this work, the viscosity and solute diffusivity is assumed to be constant. To evaluate the sensitivity of the axial development of gel concentration and transmembrane flux to these variables, parametric studies were performed for a wide range of operating conditions common in UF systems.

The variations of transmembrane flux and surface solute concentration along the length of the membrane module are shown in Figs. 1(a,b) for feed flow rates, u_0 ranging from 35 to 95 cm/s, respectively. In this simulation, the values of the parameters used are: transmembrane pressure, $\Delta p_0 = 10$ kg/cm^2; feed concentration, $c_0 = 1$ %w, and solute rejection coefficient, $\beta = 1.0$. As shown in Fig. 1(a), the transmembrane flux decreases along the axial position at all feed flow rates, but an increase in feed rate results in higher flux. The surface solute concentration increases along the length for all feed flow rates, which is illustrated in Fig. 1(b). Under the flow condition, the flow in tubular module was always laminar. In flow systems, the thickness of hydrodynamic and concentration boundary layer decreases with increasing flow rates. Thus, an increase in flow rate reduces the polarization effect with consequent reduction in surface solute concentration. This expected behavior is shown in Fig. 1(b).

For a given set of operating conditions, the feed concentration has a profound effect on transmembrane flux. The axial variation of transmembrane flux and surface solute concentration are shown in Figs. 2(a,b) for feed composition varied from 0.1 to 1.0 %w, respectively. The operating conditions used in this simulation are: transmembrane pressure, $\Delta p_0 = 10$ kg/cm^2; feed flow rate, $u_0 = 55$ cm/s, and solute rejection coefficient, $\beta = 1.0$. The surface solute concentration increases along the length at all feed concentrations, while the

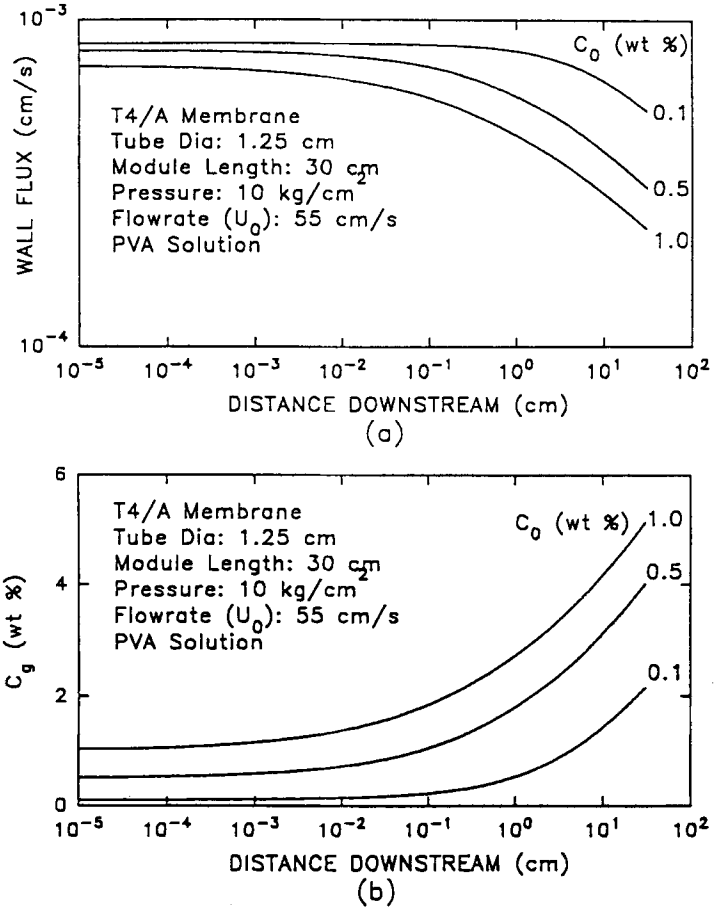

FIGURE 2: Axial variation of (a) transmembrane flux, and (b) solute concentration at the membrane wall with feed concentration (c_o) as a parameter.

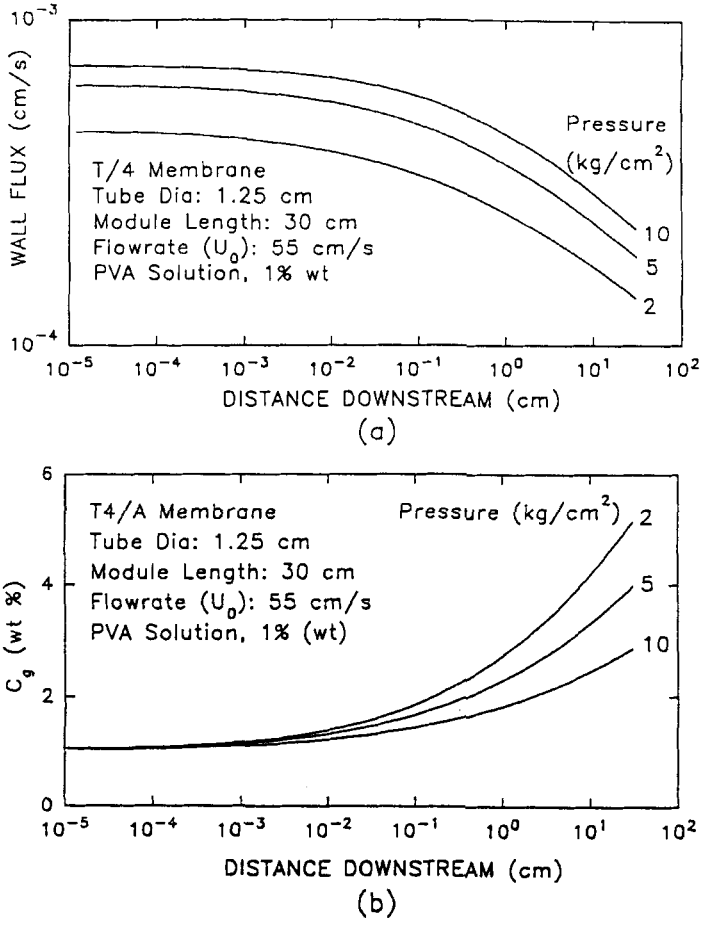

FIGURE 3: Axial variation of (a) transmembrane flux, and (b) solute concentration at the membrane wall with pressure (p) as a parameter.

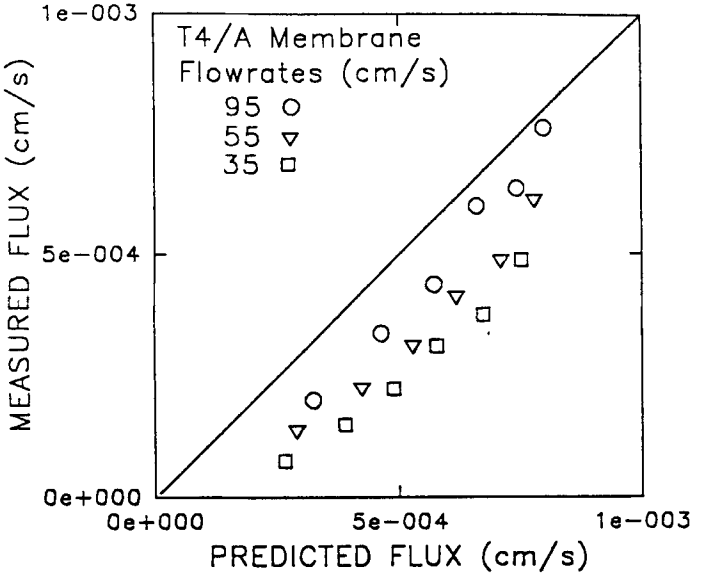

FIGURE 4: A comparison of measured flux of PVA aqueous solution (0.001-1.0 wt%) with model prediction.

permeate flux decreases. For a finite length of the membrane, an increase in feed concentration slightly increases the surface solute concentration along the axial position, as shown in Fig. 2(b). However, the permeate flux is greatly affected by the feed concentration. In Fig. 2(a), the effect of feed concentration on permeate flux is illustrated, which clearly shows that an increase in feed concentration results in lower transmembrane flux.

The effect of operating pressures on permeate flux and surface solute concentration is shown in Figs. 3(a,b). The conditions used for this case are: feed concentration, $c_0=1$ %w, feed flow rate, $u_0=55$ cm/s, and solute rejection coefficient, $\beta=1.0$, with transmembrane pressure, Δp_0 varying from 2 to 10 kg/cm^2. For a finite length of the module, an increase in operating pressure results in a slight increase in surface solute concentration. In fact, one would observe a substantial improvement of transmembrane flux without any relief in surface solute concentration. This is illustrated in Figs. 3(a,b).

In Fig. 4, comparisons of average measured flux with model prediction are shown for three feed rates. The experimental data were taken from Nakao,

et al. (32). Experiments were carried out in a tubular ultrafiltration unit (cellulose acetate membrane, T4/A) with PVA 224 aqueous solution. The effective length of the module was 30 cm and the inside diameter of the tubular membranes was 1.25 cm. The feed flow rates were in the range of 35 to 95 cm/s with operating transmembrane pressure varying from 2 to 10 kg/cm^2. The model included the effect of gel polarization resistance, as given by Eq. 35. It appears that the model tends to overestimate the measured flux. If the gel-polarization effect is neglected, the model will grossly overestimate the measured flux. The transmembrane flux depends on four parameters: resistance of the membrane, resistance of the gel-polarization layer, transmembrane pressure and the osmotic pressure. In this work, due to non-availability of osmotic pressure data for PVA aqueous solution, the effect of osmotic pressure was neglected. As it can be seen by inspection of Eq. 13, the inclusion of osmotic pressure in the model would result in reduced transmembrane flux. Thus, with the inclusion of osmotic pressure effect in the model (assuming concentration-dependent osmotic data is available) one would expect to predict the measured flux closely.

CONCLUSIONS

The present study provides fundamental understanding of concentration polarization in ultrafiltration systems. The modeling of the system requires solution of coupled transport equations of momentum and solute continuity. The equations have been solved by an implicit finite-difference method. The model requires prior knowledge of membrane permeability, kinematic viscosity and density of feed solution, solute diffusivity and concentration-dependent osmotic pressure data (if available). In the absence of gel-polarization, membrane permeability is assumed constant and may be obtained from pure solvent flux data. In the case of gel polarization, the effect of surface solute concentration on the transmembrane flux is accounted for by including the resistance of the gel layer as a function of solute concentration at the membrane surface, as outlined by Nakao, et al. (32). The input specifications are feed flow rate, feed concentration and inlet transmembrane pressure drop. The model does not require any specification of overall axial pressure drop. The wall permeation flux, surface solute concentration and pressure drop along the axial length are computed as a part of the iterative solution of the coupled momentum and solute continuity equations.

From the present simulation studies, it is now possible to evaluate the effect of such variables as feed flow rate, feed concentration, solute diffusivity, kinematic viscosity and density of feed solution, operating pressure, and

membrane permeability (with or without gel-polarization effect) on concentration polarization in tubular ultrafiltration. This allows one to evaluate the performance of ultrafiltration systems for given operating and feed conditions without decoupling the transport equations and may also provide a useful tool to optimize operating conditions. The present model can be readily extended to hollow-fiber and thin-channel ultrafiltration systems.

NOMENCLATURE

A	membrane area, cm^2
A_j	coefficient of $U_{i,j-1}$ of Eq. 21 as defined by Eq. 23
A_m	membrane permeability, $cm \cdot s^{-1}/kg \cdot cm^{-2}$
B_j	coefficient of $U_{i,j}$ of Eq. 21 as defined by Eq. 24
c	concentration of solute, %w
C	dimensionless solute concentration, c/c_0
C_g	dimensionless surface solute concentration, c_g/c_0
c_g	surface solute or gel concentration, %w
c_0	feed concentration, %w
D_e	solute diffusivity, $cm^2 \cdot s^{-1}$
D_j	coefficient of $U_{i,j+1}$ of Eq. 21 as defined by Eq. 25
DR	as defined in Eq. 31
DR1	as defined in Eq. 31
DR2	as defined in Eq. 31
E_j	a constant in Eq. 21 as defined by Eq. 26
F_j	coefficient of $C_{i,j-1}$ of Eq. 22 as defined by Eq. 27
G_j	coefficient of $C_{i,j}$ of Eq. 22 as defined by Eq. 28
H_j	coefficient of $C_{i,j+1}$ of Eq. 22 as defined by Eq. 29
I_j	a constant in Eq. 22 as defined by Eq. 30
J	average permeate flux, $cm \cdot s^{-1}$
p	pressure, $kg \cdot cm^{-2}$
p_o	pressure on the permeate side, $kg \cdot cm^{-2}$
Δp	transmembrane pressure, $(p-p_o)$, $kg \cdot cm^{-2}$
Δp_0	initial transmembrane pressure, $kg \cdot cm^{-2}$
ΔP	dimensionless transmembrane pressure, $2(p-p_o)/\rho u^2_{0,avg}$
Pe_{w0}	Peclet number based on initial wall flux, $v_{w0}r_i/D$
Q_t	filtrate volume at time t, cm^3
r	radial direction
r_i	inside radius of tubular membranes, cm
r_m	effective membrane resistance, $kg \cdot cm^{-2}/cm \cdot s^{-1}$
r_{mf}	resistance of fouling layer, $kg \cdot cm^{-2}/cm \cdot s^{-1}$
r_{mw}	membrane resistance based on pure water flux, $kg \cdot cm^{-2}/cm \cdot s^{-1}$
r_p	resistance of polarization layer, $kg \cdot cm^{-2}/cm \cdot s^{-1}$

$r_{p\delta}$ resistance of concentration boundary layer, $kg \cdot cm^{-2}/cm \cdot s^{-1}$
r_{pg} resistance of gel layer, $kg \cdot cm^{-2}/cm \cdot s^{-1}$
R dimensionless radial direction, r/r_i
R_m normalized effective membrane resistance, $2v_{w0}r_m/\rho u^2_{0,avg}$
R_p normalized gel-polarization layer resistance, $2v_{w0}r_m/\rho u^2_{0,avg}$
Re_{w0} wall Reynolds number based initial wall flux, $v_{w0}r_i/\nu$
s compressibility exponent of the cake, dimensionless
t time, s
u axial velocity component in z-direction, $cm \cdot s^{-1}$
u_0 inlet velocity at z=0, $cm \cdot s^{-1}$
$u_{0,avg}$ average inlet velocity, $cm \cdot s^{-1}$
U dimensionless axial velocity, $u/u_{0,avg}$
U_0 dimensionless velocity at the module inlet, $u_0/u_{0,avg}$
v velocity in r-direction, $cm \cdot s^{-1}$; in Eqs. 1-2, v is velocity vectors
v_{w0} initial wall flux, $cm \cdot s^{-1}$
V dimensionless radial velocity, v/v_{w0}
w weight of particulate per unit volume of filtrate, $g \cdot cm^{-3}$
z axial direction
Z dimensionless axial direction, $v_{w0}z/u_{0,avg}r_i$
β solute rejection coefficient at the membrane surface
ν kinematic viscosity of feed solution, $cm^2 \cdot s^{-1}$
μ dynamic viscosity, $g \cdot cm^{-1} \cdot s^{-1}$
π osmotic pressure of the solute in solution, $kg \cdot cm^{-2}$
π_o osmotic pressure of permeate, $kg \cdot cm^{-2}$
$\Delta\Pi$ transmembrane osmotic pressure, $2(\pi-\pi_o)/\rho u^2_{0,avg}$
ϕ dynamic membrane constant, $(kg \cdot cm^{-2})^{-s} \cdot g^{-1}$
ρ density of feed solution

REFERENCES

1. M. Cheryan, *Ultrafiltration Hand Book*, Technomic Publishing Inc., Pennsylvania (1986).

2. C.A. Smolders, and Th. van den Boomgaard, *J. Memb. Sci.*, **40**, 121 (1989).

3. R.L. Merson, and D.N. Lee, *J. Food Sci.*, **41**, 403 (1976).

4. A. Suki, A.G. Fane, and C.J.D. Fell, *J. Memb. Sci.*, **21**, 269 (1984).

5. H. Reihanian, C.R. Robertson, and A.S. Michaels, *J. Memb. Sci.*, **16**, 237 (1983).

6. R.B. Bird, W.E. Stewart, and E.N. Lightfoot, *Transport Phenomena*, John Wiley, New York (1960).

7. L. Dresner, *Oak Ridge Natl. Lab.*, Report 3621 (1964).

8. R.E. Fisher, T.K. Sherwood, and P.L.T. Brian, *MIT Desalination Res. Lab.*, Report 295-5 (1964).

9. T.K. Sherwood, P.L.T. Brian, R.E. Fisher, and L. Dresner, *Ind. Eng. Chem. Fund.*, **4**, 113 (1965).

10. P.L.T. Brian, *Ind. Eng. Chem. Fund.*, **4**, 439 (1965).

11. W.N. Gill, C. Tien, and D.W. Zeh., *Ind. Eng. Chem. Fund.*, **4**, 433 (1965).

12. A.S. Berman, *J. Appl. Phys.*, **24**, 1232 (1953).

13. W.N. Gill, L.J. Derzansky, and M.R. Doshi, "Convective Diffusion in Laminar and Turbulent Hyperfiltration (Reverse Osmosis) Systems," *Surface and Colloid Science*, E. Matijevic (ed.), Wiley, New York, **4**, 261, (1971).

14. J.S. Johnson, and J.W. McCutchan, *Desalination*, **10**, 147 (1972).

15. C.A. Hieber, *Desalination*, **15**, 59 (1974).

16. W-F. Leung, and R.F. Probstein, *Ind. Eng. Chem. Fund.*, **18**, 274 (1979).

17. M.R. Doshi, and W.N. Gill, *Chem. Eng. Sci.*, **30**, 467 (1975).

18. C.C. Hung, and C. Tien, *Desalination*, **18**, 173 (1976).

19. C.Y. Chang, and J.A. Guin, *AIChE J.*, **24**, 1046 (1978).

20. C. Kleinstreuer, and Paller, M.S., *AIChE J.*, **29**, 529 (1983).

21. R.P. Ma, C.H. Gooding, and W.K. Alexander, *AIChE J.*, **31**, 1728 (1985).

22. W.N. Gill, D.E. Wiley, C.J.D. Fell, and A.G. Fane, *AIChE J.*, **34**, 1563 (1988).

23. U. Merten, *Ind. Eng. Chem. Fund.*, **2**, 229 (1963).

24. M.C. Porter, "Membrane Filtration," *Handbook of Separation Techniques for Chemical Engineers*, P.A. Scheweitzer (ed.), 2-1, McGraw-Hill, New York (1979).

25. J.A. Howell, and D. Velicangil, *J. Appl. Polymer Sci.*, **27**, 21 (1982).

26. A.G. Fane, *J. Memb. Sci.*, **20**, 249 (1984).

27. S. Ilias, and R. Govind, *J. Memb. Sci.*, **39**, 125 (1988).

28. A.G. Aboulnour, H.A. Talat, M.H. Sorour, and S.R. Tewfik, *Desalination*, **68**, 35 (1988).

29. R.W. Baker, and H. Strathmann, *J. Appl. Polymer Sci.*, **14**, 1197 (1970).

30. W.F. Blatt, A. Dravid, A.S. Michaels, and L. Nelsen, "Solute Polarization and Cake Formation in Membrane Ultrafiltration: Causes, Consequences and Control Techniques," *Membrane Science and Technology*, J.E. Flinn (ed.), 47, Plenum Press, New York (1970).

31. M.C. Porter, *Ind. Eng. Chem. Product Research Develop.*, **11**, 234 (1972).

32. S-I. Nakao, T. Nomura, and S. Kimura, *AIChE J.*, **25**, 615 (1979).